View metadata, citation and similar papers at core.ac.uk

brought to you by CORE

provided by Aaltodoc Publication Archive

Aalto University

Aaltodoc

OPEN ACCESS

This is an electronic reprint of the original article.
This reprint may differ from the original in pagination and typographic detail.

Author(s): Lotkhov, Sergey V. & Saira, Olli-Pentti & Pekola, Jukka & Zorin, Alexander B.

Title: Single-charge escape processes through a hybrid turnstile in a dissipative environment

Year: 2011

Version: Final published version

Please cite the original version:

Lotkhov, Sergey V. & Saira, Olli-Pentti & Pekola, Jukka & Zorin, Alexander B. 2011. Single-charge escape processes through a hybrid turnstile in a dissipative environment. New Journal of Physics. Volume 13, Issue 1. 013040/1-14. ISSN 1367-2630 (printed). DOI: 10.1088/1367-2630/13/1/013040.

Rights: © 2011 IOP Publishing. This is the accepted version of the following article: Lotkhov, Sergey V. & Saira, Olli-Pentti & Pekola, Jukka & Zorin, Alexander B. 2011. Single-charge escape processes through a hybrid turnstile in a dissipative environment. New Journal of Physics. Volume 13, Issue 1. 013040/1-14. ISSN 1367-2630 (printed). DOI: 10.1088/1367-2630/13/1/013040, which has been published in final form at http://iopscience.iop.org/1367-2630/13/1/013040. This work is distributed under the Creative Commons Attribution 3.0 License (https://creativecommons.org/licenses/by/3.0/).

All material supplied via Aaltodoc is protected by copyright and other intellectual property rights, and duplication or sale of all or part of any of the repository collections is not permitted, except that material may be duplicated by you for your research use or educational purposes in electronic or print form. You must obtain permission for any other use. Electronic or print copies may not be offered, whether for sale or otherwise to anyone who is not an authorised user.

IOPscience iopscience.iop.org

Home Search Collections Journals About Contact us My IOPscience

Single-charge escape processes through a hybrid turnstile in a dissipative environment

This content has been downloaded from IOPscience. Please scroll down to see the full text.

2011 New J. Phys. 13 013040

(http://iopscience.iop.org/1367-2630/13/1/013040)

View the table of contents for this issue, or go to the journal homepage for more

Download details:

IP Address: 130.233.216.27

This content was downloaded on 27/05/2015 at 07:24

Please note that terms and conditions apply.

New Journal of Physics
The open-access journal for physics

Single-charge escape processes through a hybrid turnstile in a dissipative environment

Sergey V Lotkhov[1,4], **Olli-Pentti Saira**[2,3], **Jukka P Pekola**[2] **and Alexander B Zorin**[1]

[1] Physikalisch-Technische Bundesanstalt, Bundesallee 100, 38116 Braunschweig, Germany
[2] Low Temperature Laboratory, Aalto University, PO Box 13500, FI-00076 Aalto, Finland
[3] Department of Applied Physics/COMP, Aalto University, PO Box 14100, FI-00076 Aalto, Finland
E-mail: Sergey.Lotkhov@ptb.de

New Journal of Physics **13** (2011) 013040 (14pp)
Received 11 October 2010
Published 26 January 2011
Online at http://www.njp.org/
doi:10.1088/1367-2630/13/1/013040

Abstract. We have investigated the static, charge-trapping properties of a hybrid superconductor–normal metal electron turnstile embedded in a high-ohmic environment. The device includes a local Cr resistor on one side of the turnstile, and a superconducting trapping island on the other side. The electron hold times, $\tau \sim 2$–20 s, in our two-junction circuit are comparable with those of typical multi-junction, $N \geqslant 4$, normal-metal single-electron tunneling devices. A semi-phenomenological model of the environmental activation of tunneling is applied for the analysis of the switching statistics. The experimental results are promising for electrical metrology applications.

[4] Author to whom any correspondence should be addressed.

1367-2630/11/013040+14$33.00
© IOP Publishing Ltd and Deutsche Physikalische Gesellschaft

Contents

1. Introduction 2
2. Fabrication and experiment 3
3. Results and discussion 5
4. Model of the environmental activation of tunneling for the R-SINIS trap 8
4.1. Environmental activation of tunneling: theoretical framework 8
4.2. Fluctuator 1: on-chip resistor 10
4.3. Fluctuator 2: a source of high-frequency noise 11
4.4. Results 11
5. Conclusions and outlook 13
Acknowledgments 13
References 14

1. Introduction

Currently, growing interest in the quantum sources of electrical current, based on a clocked transfer of the elementary charges, is observed to exist. Developed for mesoscopic systems of small tunnel junctions, an orthodox theory of single-electron tunneling (SET) [1] has been used to describe the operation of the SET pumping devices (for a few examples, see [2]–[4]) in terms of cyclic sequences of the charge states with the charge values on the nodes being a multiple of the electron charge $e \approx 1.602 \times 10^{-19}$ C. The quantized current value is given by $I = k \times ef$, where f is the cycling frequency and k the number of electrons transferred in one cycle.

A more complete picture involves a broad scope of cotunneling leakage processes [5, 6] as well as the influence of the electromagnetic environment [7, 8] to explain the finite, often unexpectedly short decay times of the participating charge configurations, imposing significant limitations on the pumping accuracy. Accordingly, the rate of charge leakage across the whole device has been an important characteristic of any Coulomb blockade circuit (see e.g. [3, 4, 9]). For example, in the quantum standard of capacitance, this insulation property was ultimately quantified by measuring a single-electron hold time of the pump in the static mode with the help of an SET electrometer [9].

In the present experiment, we address the insulation properties of a novel single-gate electron turnstile, recently realized as a hybrid SET transistor, built on two superconductor–insulator–normal metal (SIN) tunnel junctions [4]. In this turnstile, the interplay of the Coulomb blockade and the sub-gap current suppression enables the accurate transfer of single electrons, using only one gate signal. A promising estimate was obtained theoretically [6, 10] for the fundamental accuracy of such a turnstile to be at the relative level of 10^{-8} for currents up to 10 pA. Parallel operation of up to ten devices driven by a common rf-gate, producing a total current above 100 pA, has been demonstrated [11]. On the other hand, having only two junctions in-series, $N = 2$, instead of, for instance [9], $N = 7$, was found to be a critical issue for the metrological applications due to non-vanishing sub-gap leakage currents, deteriorating the pumping performance.

It has been predicted theoretically [12, 13] and proven experimentally [14]–[16] that for few-junction normal-state SET circuits, there is an efficient way of suppressing the cotunneling leakage through engineering the electromagnetic environment of the junctions. Quantitatively,

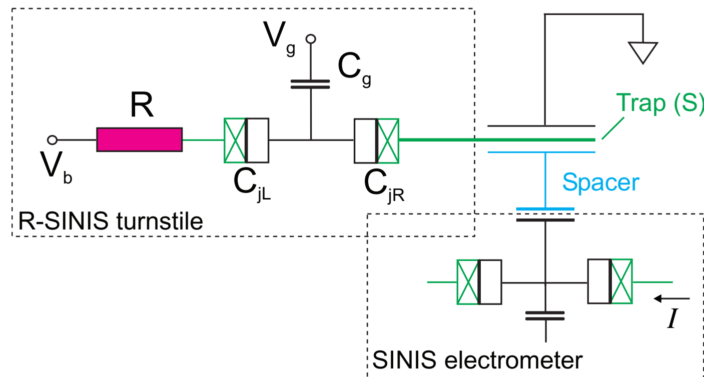

Figure 1. Equivalent circuit of the sample, including an R-SINIS turnstile and trapping island coupled capacitively via a spacer electrode to a SINIS electrometer. The open/crossed boxes indicate the normal/superconducting electrodes of the tunnel junction.

the implementation of an in-series high-ohmic local resistor R provides a result similar to an extension of the series array by n additional tunnel junctions, where $n \sim R/R_Q$ and $R_Q \equiv h/e^2 \approx 25.8\,\mathrm{k}\Omega$ is the resistance quantum. For example, the hold times in a four-junction R-trap (array with the resistor $R \approx 50\,\mathrm{k}\Omega$) on the scale of hours [15] were found comparable to those for 7 to 9-junction traps without resistors [17, 18].

Compared to the normal-state case, there is a possibility of an additional first-order error process in the hybrid turnstile that involves tunneling of electrons, either photon assisted [8] or via the Dynes density of sub-gap states [19]. However, even in this case, a high-ohmic environment can be helpful in reducing the leakage. In the previous experiment on R-turnstiles (a hybrid turnstile connected in series to the resistors, see [20]), we were able to achieve more than an order of magnitude suppression of the sub-gap current.

Rapid progress in understanding the sub-gap tunneling phenomena as well as the efficient methods [8, 20], developed for their suppression, brought the frontier of experiments down to a single-electron level [21] and the current uncertainty: much closer to the level demanded by metrology. In this work, we report on the behavior of the R-turnstile in the static hold mode, i.e. in the configuration where it is connected to a small 'trapping' island monitored by an SET electrometer. The hold times, measured in our experiment on the scale up to $\tau \sim 20\,\mathrm{s}$, are promising for metrological applications, due to exceptionally low sub-gap current uncertainty $\Delta I \sim e/\tau \sim 10^{-20}\,\mathrm{A}$. The electron switchings are analyzed along the lines of the model of environmental activation of tunneling, proposed in previous works [8, 21].

2. Fabrication and experiment

The experimental circuit is shown in figure 1. It includes a hybrid SINIS-type R-turnstile, terminated by the trapping island capacitively coupled to an SINIS SET electrometer. An SEM image of the structure is shown in figure 2. It was fabricated on the thermally oxidized Si substrate by means of the standard shadow evaporation technique [22]. The layout consists of three replicas of different materials: Cr for the resistor, 12 nm-thick, evaporated in oxygen

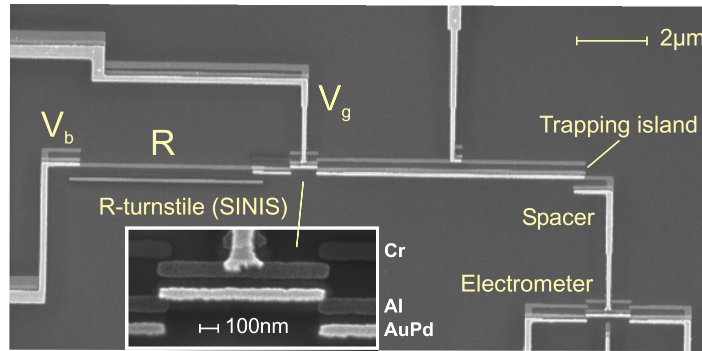

Figure 2. SEM picture of the experimental structure. The inset shows a close-up of the double-junction structure of the turnstile.

Table 1. Estimates of the sample parameters. Here, $R_T = R_T^{\mathrm{left}} = R_T^{\mathrm{right}}$ is a junction resistance in the turnstile, $E_C \equiv e^2/[2 \times (C_{jL} + C_{jR} + C_g)]$ the turnstile charging energy and $\tau_{\max}$ the maximum expectation value of the hold time.

Sample no.	R_T (kΩ)	E_C (μeV)	Δ_{Al} (μeV)	$R(0)$ (kΩ)	$R(\infty)$ (kΩ)	$\tau_{\max}$ (s)
1	600	750	260	85	44	25.0
2	120	360	230	38	36	2.6

at a pressure of about 1.5×10^{-4} Pa; Al (18 nm) oxidized just after the evaporation at 1 Pa for 5 min to form the tunnel barrier; and a proximity bilayer of Al (5 nm) and AuPd (20 nm), building together the normal-state island of the turnstile. Here, the thin Al film was used in order to improve the quality of the tunnel barrier. For the purpose of increasing the yield of the intact junctions, the layout included a semiconducting ring of evaporated Si (not shown), cross-connecting all on-chip lines during sample manipulations at room temperature [23].

The trapping island was made of solely the superconducting Al, to avoid unpaired electron states within the energy gap Δ. The island was coupled to the electrometer indirectly through its capacitive link to the neighboring normal-conducting replica, connected galvanically to a spacer electrode, as shown in figure 2. Due to the indirect way of coupling, the electrometer response function was sufficiently weak to avoid the back influence of this charge detector on the trap (see below).

The measurements were carried out in a dilution fridge with a base temperature of 15 mK. The sample was encapsulated in a microwave-tight but not vacuum-sealed sample holder. Thermocoax$^{\mathrm{TM}}$ coaxial filters, approximately 1–1.5 m long, were installed into the sample holder for every signal line. One exception was, however, made for the high-frequency gate line (used in the present experiment to apply a dc voltage V_g), equipped with a much shorter coaxial filter, about 5 cm.

The results of this paper are demonstrated on two samples with substantially different parameters, determined with the help of relevant test devices and summarized in table 1. We note that, due to high oxygen content, our resistive Cr lines exhibited slightly nonlinear *IV* curves, characterized by the different zero-bias and asymptotic resistances $R(0) \gtrsim R(\infty)$.

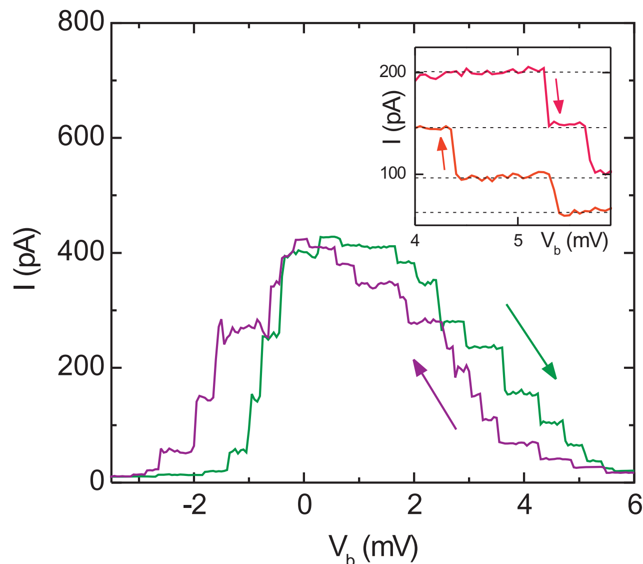

Figure 3. A step-like response of the electrometer signal to the single-quasiparticle charging in sample 1. For this sweep, the continuous polarization of the trapping island is permanently canceled by a gate signal $\delta V_g = -0.8 \times \delta V_B$. The trapping effect gives rise to a hysteretic displacement of the curve should the sweep direction be reversed. The notable irregularity of the state transitions appears due to the stochastic nature of the switching processes studied in this work. Inset: a hysteresis loop indicating quasistability of up to three charge states.

3. Results and discussion

An important manifestation of the trapping effect is hysteresis, appearing in the charge detector response, as we reverse the direction of charging the trap, see figure 3. A single-electron trapping induced a small polarization charge on the electrometer island, corresponding to 1/24th part of the modulation period, as shown in part by a step-like modulation function in figure 3. During the voltage sweep V_b in figure 3, we applied a cross-talk cancelation signal to the gate V_g, which was used to counterbalance the continuous voltage modulation of the trapping island and the electrometer island. As a result, the discrete detector signal was observed, due to electron tunneling events only, as manifested in the inset to figure 3 by a stepped shape of the hysteresis loops.

As previously mentioned, the detection of incremental charging of the trapping island was done by means of a voltage-biased SINIS transistor. In order to obtain a measurable output current, the bias voltage was increased above the gap value, $V_{EM} > 2\Delta/e$, which is sufficiently high to enable appreciable quasiparticle current. Accordingly, one could expect significant disturbances, imposed on the trap by the quasiparticle recombination processes in such a detector. However, as shown in figure 4, the frequency of random switchings in the trap was not noticeably affected within the practical range of the electrometer currents, $I \sim 500$ pA.

Since, depending on the voltage settings, both one-electron and two-electron (Andreev reflections) tunneling events can, in principle, contribute to the detector signal, we first

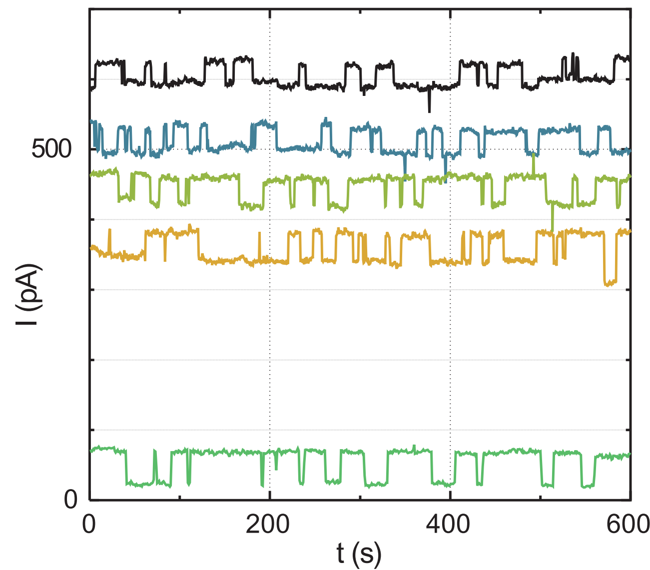

Figure 4. Random state switchings in sample 1, detected by the electrometer, biased to five different operation points and thus related to different levels of the dissipated power $P \equiv I \times V_{EM}$, V_{EM} being the bias voltage of the detector. From the bottom to the top: $P \approx 0.03, 0.32, 0.44, 0.53$ and 0.66 pW. The corresponding lifetime expectations, $\tau = 25$, 17.1, 17.6, 15.4 and 19.3 s, indicate only a weak influence of the electrometer on the trapping circuit.

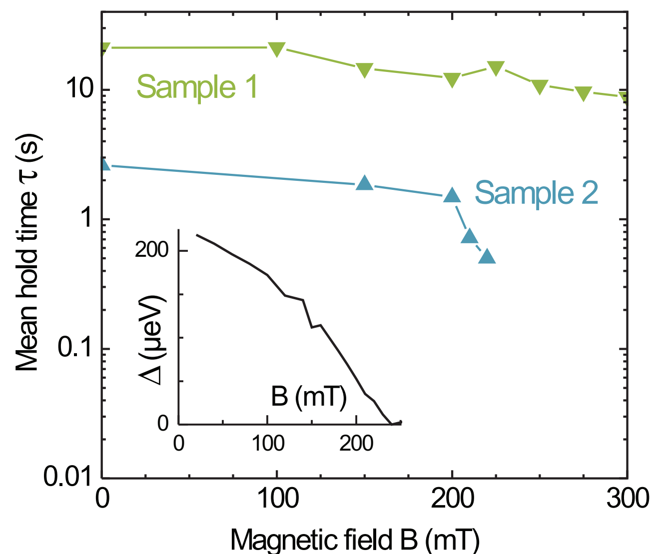

Figure 5. Average hold time as a function of the magnetic field for samples 1 and 2. Inset: a typical dependence of the superconducting energy gap Δ of our Al film on the perpendicular magnetic field B, measured on another sample.

calibrated the experimental circuit, by driving the sample into the normal state and monitoring the single-electron switchings. In figure 5, the dependence is shown of the average hold time on the magnetic field B, arranged perpendicular to the substrate. The inset illustrates a suppression

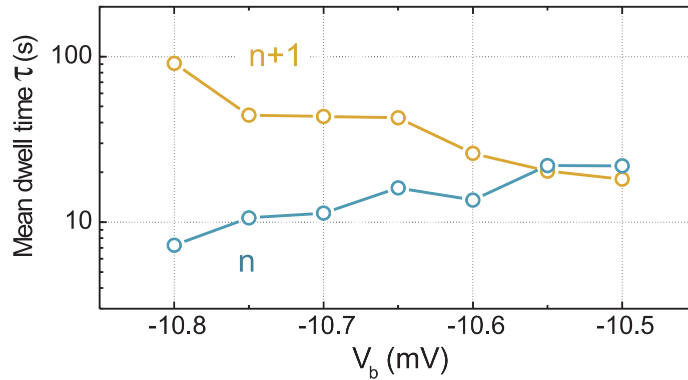

Figure 6. Average hold time as a function of voltage V_b, measured for two neighboring states with n and $n+1$ trapped electrons. The point $V_{b0} \approx -10.55$ mV corresponds to a center of the hysteresis loop (a zero-bias point). The points to the left of this symmetry point depict the hold times in the finite-bias states of the turnstile.

of the energy gap Δ with increasing values of B. The comparison with the normal-state behavior brought us to the conclusion that the majority of the events were related to 1e-tunneling even in the superconducting state. Rare 2e-events were also observed, but they were statistically indistinguishable from a possible small amount of time-unresolved two-electron tunneling sequences. On the other hand, theoretically, a single-electron escape through the SINIS turnstile must leave behind a quasiparticle excitation in the trapping island. This process is, however, prohibited energetically at low bias voltage and low temperatures. Therefore, the observation of predominantly single-electron events in our experiment must be attributed to the dominance of non-equilibrium carriers in the escape processes.

The average hold times of two equally populated neighboring charge states were registered to be at the level of $\tau \approx 20$ s, in the high-E_C energy sample 1, and $\tau \approx 2.6$ s, in the moderate-E_C sample 2. These values are remarkable, because such long hold times have been previously observed only for single-electron arrays without resistors with the number of junctions $N \geqslant 4$ (see [24]–[26]).

Due to the gate modulation by the cancelation signal δV_g (see above), a strong systematic variation of the loop width was observed, as we swept over more than ~10 loops. However, for the hold times measurements, we focused on the loop of the maximum width, where only a little change to the neighboring loops was observed. Due to the cross-talk cancelation signal, an effective bias voltage across the R-SINIS-turnstile-part of the circuit, which is zero in the center of the loop V_{b0}, can be tuned directly within the same loop as $(V_b - V_{b0})$. The latter consideration enables a direct estimate of the practical accuracy of the turnstile at finite bias voltage with the help of the data shown in figure 6. One can see that for half of the gap voltage, which typically corresponds to an optimal bias in the center of the pumping plateau [4, 20], the electron leak is still on the scale of one electron per 10 s. Accordingly, for the R-turnstile driven by a rectangular signal [10], i.e. flipped quickly between two optimized gate settings, one could expect a leakage-limited accuracy, say, at the pumping frequency $f = 10$ MHz, on the metrological level 10^{-8}.

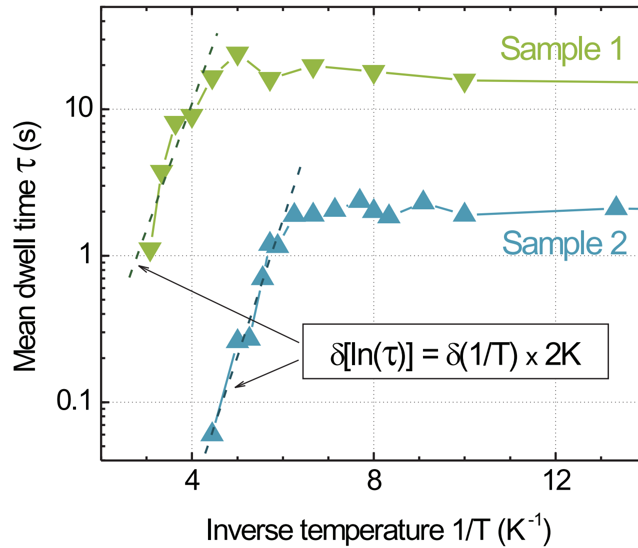

Figure 7. Average hold time as a function of the inverse temperature for samples 1 and 2. A rough comparison with the Arrhenius plot reveals qualitatively no correlation of the high-temperature slopes with E_C (differing for these samples by as much as a factor of two). See text for further details.

Furthermore, our samples demonstrated no deterioration of the hold time τ within wide temperature ranges up to 150–200 mK (see figure 7). This predicts excellent stability against the electron overheating effects for pumping currents up to ∼100 pA [27]. At higher temperatures, a fast exponential reduction of the hold times was observed. A slope of the decay, estimated in figure 7 to be similar for both samples, reveals a phenomenological activation energy of about $(k_B \times 2\,\mathrm{K})$, which is considerably lower than $E_c + \Delta$ in either sample. Our numerical analysis, which we address below, indicates that these deviations from the simple Arrhenius model of an autonomous SET trap, which basically assumes a strong dependence of τ on E_c (cf e.g. [17, 18]), appear due to the influence of the on-chip resistor and the shape of the BCS density of states in the superconductor.

4. Model of the environmental activation of tunneling for the R-SINIS trap

To facilitate the understanding of the observed escape processes, we have applied a semi-phenomenological model of environmentally enhanced tunneling in the R-SINIS trap, which assumes that a considerable noise contribution arrives from the warmer parts of the electromagnetic circuitry. Further details of this environmental activation of tunneling (EAT) approach can be found elsewhere [8, 21].

4.1. Environmental activation of tunneling: theoretical framework

Our modeling of electron escape from the trap is based on the environmental activation of single-particle tunneling events. The theoretical framework is that of standard $P(E)$ theory [28], which accounts for the photon exchange with the tunnel junction, due to the excitation of the

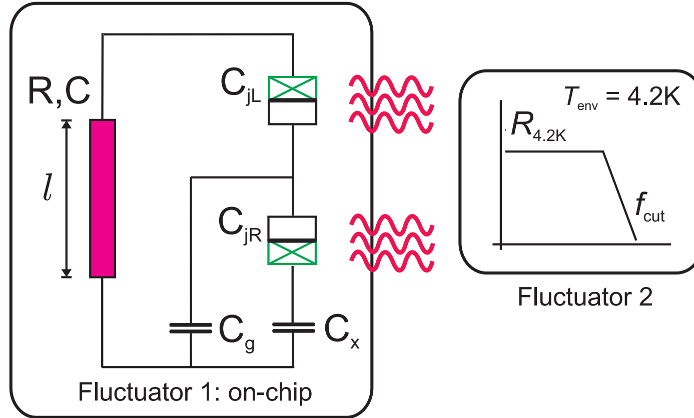

Figure 8. Schematic representation of the two-fluctuator model used in simulations. The circuit diagram to the left was used for evaluating the $P(E)$ function related to the on-chip resistor (fluctuator 1). The right-hand part of the plot shows symbolically a 'warmer' fluctuator 2.

environmental modes. Our model of the electromagnetic environment of the trap junctions includes two independent fluctuators, as shown symbolically in figure 8:

Fluctuator 1 represents our well-characterized on-chip chromium resistor, which we model as an RC transmission line at the sample stage temperature. A similar case, a first-order tunneling in the presence of on-chip resistors, has been modeled successfully with $P(E)$ theory in earlier work [29, 30].

Fluctuator 2 accounts for the high-frequency noise originating possibly from a source external to the sample stage and having higher temperature. Activation of first-order tunneling by high-temperature environment, $k_B T_{env} \gtrsim \Delta + E_c$, has been previously shown to reproduce the experimentally observed finite sub-gap conductance of NIS junctions [8], and low-temperature saturation of tunneling rates in an NIS single-electron box [21].

In the framework of $P(E)$ theory [28], an SET rate is derived on the basis of the absorption/emission spectrum of the environment, the function $P(E)$. For Gaussian fluctuators, $P(E)$ can be evaluated as

$$P(E) = \frac{1}{2\pi\hbar} \int_{-\infty}^{\infty} \mathrm{d}t \exp\left(J(t) + \frac{\mathrm{i}}{\hbar} E t\right), \tag{1}$$

where $J(t)$ is a linear phase–phase correlation function, introduced in [28] to describe fluctuations of voltage across the tunnel junction. In the case of a linear environment in thermal equilibrium, which can be characterized by an impedance $Z(\omega)$, connected in parallel to the junction of capacitance C_j, $J(t)$ equals

$$J(t) = 2\int_0^{\infty} \frac{\mathrm{d}\omega}{\omega} \frac{\mathrm{Re} Z_t(\omega)}{R_K} \times \left\{\coth\left(\frac{1}{2}\beta\hbar\omega\right)[\cos(\omega t) - 1] - \mathrm{i}\sin(\omega t)\right\}, \tag{2}$$

where $Z_t(\omega) = [Z^{-1}(\omega) + \mathrm{i}\omega C_j]^{-1}$ is the total impedance seen over the junction and $\beta \equiv (k_B T_{env})^{-1}$ is the inverse temperature of the environment. In order to describe the experimental setup, we will generalize the above result to the two-fluctuator model, where the

Table 2. Sample parameters related to fluctuator 1 and the inferred capacitive voltage division factors $\xi_{L(R)}$.

Sample	l (μm)	R (kΩ)	C (aF)	$C_{jR,L}$ (aF)	C_g (aF)	C_x (aF)	C_t (aF)	ξ_L	ξ_R
1	5	85[a]	320	40	30	100	24	0.58	0.29
2	5	38	320	100	30	100	44	0.44	0.28

[a]Zero-bias resistance $R(0)$ was used instead of the asymptotic value $R(\infty) = 44\,\mathrm{k}\Omega$.

voltage fluctuations caused by the independent fluctuators are additive. Consequently, the total $P(E)$ function can be found as a convolution

$$P(E) = \int_{-\infty}^{+\infty} \mathrm{d}E' P_1(E - E')P_2(E') \tag{3}$$

of the partial $P_{1,2}(E)$ functions, evaluated independently for the two components (cf e.g. [31]).

For a description of filtering and voltage division effects, we allow for an arbitrary transfer function $A(\omega)$, which relates the fluctuating current $I_N(\omega)$ through the impedance $Z(\omega)$ to the voltage $V(\omega)$ across the junction, so that $I_N(\omega) = A(\omega)V(\omega)$. The actual phase fluctuations across the junction will then be equivalent to those across an effective total impedance

$$Z_t^{-1}(\omega) = A(\omega)\frac{\mathrm{Re}[A(\omega)]}{\mathrm{Re}[Z^{-1}(\omega)]}, \tag{4}$$

which can be used for calculations of the $P(E)$ function with the help of equations (1) and (2).

4.2. Fluctuator 1: on-chip resistor

For evaluating $P_1(E)$ corresponding to the on-chip resistor, we will use the reduced circuit diagram, shown in detail in the left-hand part of figure 8. R and C denote the total capacitance of the Cr wire, and $r = R/l$ and $c = C/l$ where l is the wire length. For c, we take a rule-of-thumb value $c = 6\epsilon_0 = 5.3 \times 10^{-11}\,\mathrm{F\,min^{-1}}$ accounting for geometric stray capacitance. We have introduced a shorthand notation $A \parallel B := (A^{-1} + B^{-1})^{-1}$ for impedance calculations. The essential RC transmission line parameters are the frequency-dependent wave number, $\alpha(\omega) = (1 + \mathrm{i})\sqrt{(\omega rc/2)}$, and the characteristic line impedance, $Z_0(\omega) = (1 - \mathrm{i})\sqrt{(r/2\omega c)}$. For a semi-infinite line, the impedance seen from the open end equals the characteristic impedance, and for a finite wire terminated with a short circuit, one finds $Z(\omega) = Z_0(\omega)\tanh[\alpha(\omega)l]$.

Next, we note that the electrical circuit in parallel with the resistor consists of purely capacitive elements only. Hence, it can be modeled by a single lumped capacitor of value $C_t = C_{jL} \parallel (C_g + C_{jR} \parallel C_x)$. The voltage fluctuations over the junctions L and R are equivalent to the fluctuations over C_t, scaled by a factor ξ accounting for the capacitive voltage division. For the left (upper) junction, we have $\xi_L = [1 + C_{jL}/(C_g + C_{jR} \parallel C_x)]^{-1}$, and for the right, $\xi_R = (1 + C_{jR}/C_x)^{-1}[1 + (C_g + C_{jR} \parallel C_x)/C_{jL}]^{-1}$. According to equation (4), voltage division by factor ξ is equivalent to scaling $Z_t(\omega)$ by a factor of ξ^2. Based on the preceding argument, we can now write the effective impedance, used for evaluating the $P_1(E)$ function related to Fluctuator 1, as

$$Z_t(\omega) = \frac{\xi^2}{\mathrm{i}\omega C_t + Z_0^{-1}(\omega)\coth[\alpha(\omega)l]}. \tag{5}$$

The numerical values of the model parameters are presented in table 2.

4.3. Fluctuator 2: a source of high-frequency noise

The principal escape mechanism is assumed to be related to the excitation of quasiparticles by the photons with energy $E_{\mathrm{ph}} \sim \Delta + E_{\mathrm{c}}$, which is high enough to overcome the Coulomb blockade in the turnstile. For both studied samples $E_{\mathrm{c}} > \Delta$, and hence the relevant noise frequencies are above $f_{\mathrm{ph}} \equiv E_{\mathrm{ph}}/h \sim 100\,\mathrm{GHz}$. The photon excitations are expected to arrive from the warmer (and more distant) parts of the environment, to be modeled as fluctuator 2, shown symbolically in the right-hand part of figure 8.

Due to the lack of microscopic understanding, we will model fluctuator 2 just as a parallel RC circuit at $T = 4.2\,\mathrm{K}$ (see previous work in [8, 21]), coupled directly to either junction. Used as a model parameter, the cut-off frequency f_{cut} of this effective circuit can be reasonably interpreted as the cut-off of the coupling between the source and the junction. Taking into account that the gate capacitances in the reported turnstiles are comparable to those of the (very small) tunnel junctions, we assume the gate lines are the dominant on-chip propagation ways for the external noise. (For simplicity, this concern was disregarded in figure 8.) In contrast, the high-frequency power attenuation for the on-chip Cr resistors is very strong: if modeled as RC transmission lines, it takes the exponential form $\exp(-\sqrt{2\omega RC})$ with the cut-off frequency $1/(2\pi RC) \sim 10\,\mathrm{GHz} \ll f_{\mathrm{ph}}$.

As long as the hold time at low temperatures depends mainly on the spectral density of environmental emission at high frequencies $\sim f_{\mathrm{ph}} \gg f_{\mathrm{cut}}$, the source resistance and cut-off frequency of the high-temperature environment cannot be independently extracted from the measurements. In the calculations, a constant cut-off frequency $f_{\mathrm{cut}} = 0.5\,\mathrm{GHz}$ was used, corresponding to the filtering properties of the Thermocoax$^{\mathrm{TM}}$ lines. We stress that the effective source resistance $R_{4.2\,\mathrm{K}}$, obtained as a model fit parameter, formally includes details of a phenomenological transfer function $A(\omega)$ and is not expected to be equal to the actual source resistance.

4.4. Results

The typical composite $P(E)$ functions, resulting from the calculations described above, are shown in figure 9. The slowly decaying environmental absorption spectrum ($E > 0$) is due to the on-chip resistor, whereas the finite emission probabilities on the millivolt scale at low temperatures stem from the high-frequency noise. A maximum of the $P(E)$ functions occurs at a positive voltage due to the dynamic Coulomb blockade arising owing to the on-chip resistor.

The SET rates were computed using the golden rule formula

$$\Gamma(U) = \frac{1}{e^2 R_{\mathrm{T}}} \int_{-\infty}^{\infty} \mathrm{d}E_1 \int_{-\infty}^{\infty} \mathrm{d}E_2\, n_{\mathrm{S}}(E_1) f_{\mathrm{S}}(E_1)[1 - f_{\mathrm{N}}(E_2)] P(E_1 - E_2 + U), \tag{6}$$

where R_{T} is the junction resistance, $n_{\mathrm{S}}(E)$ the density of states in the S electrode and $f_{\mathrm{N(S)}}$ the occupation factor for quasiparticle states in the N (S) electrode. In our model, we use the pure BCS density of states $n_{\mathrm{S}}(E) = |\mathrm{Re}(E/\sqrt{E^2 - \Delta^2})|$ and the occupation factors are taken to obey equilibrium Fermi distribution, i.e. $f_{\mathrm{N,S}}(E) = [1 + \exp(E/k_{\mathrm{B}}T)]^{-1}$, where T is the sample stage temperature. The assumption of the equilibrium quasiparticle distribution in the S electrodes is based on the ultra-low injection rates (of the order of 1 Hz), allowing for sufficiency of the quasiparticle relaxation/recombination rates on both sides of the turnstile. The tunneling rates $\Gamma_{\mathrm{L(R)}}$ were evaluated independently for the left and right tunnel junctions, respectively.

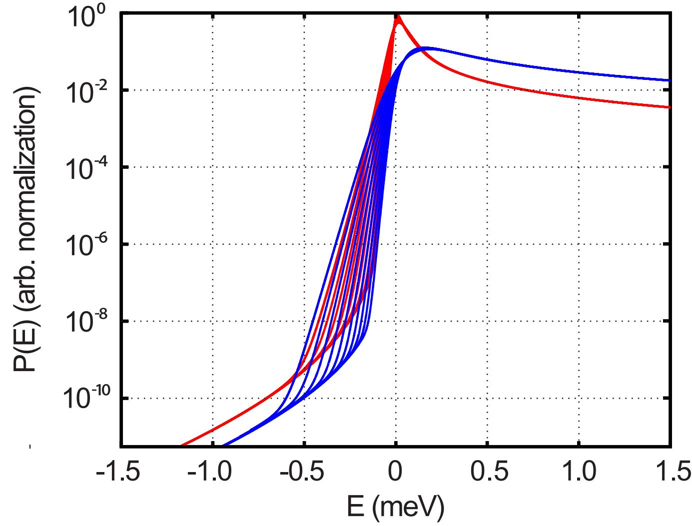

Figure 9. $P(E)$ curves calculated with respect to the junctions L (blue curves) and R (red curves), for the parameters of sample 1 (see table 2) and various temperatures in the range of 50–300 mK (in the order of broadening of the peak toward the higher temperatures).

Table 3. Sample parameters accepted for the final evaluation of the hold times in figure 10.

Sample	R_T (kΩ)	Δ (μeV)	E_c (μeV)	$R_{4.2\,K}$ (Ω)
1	600	260	600	11.3
2	120	230	360	1.8

Finally, the hold times τ were calculated based on the master equation [1] for SET:

$$\tau^{-1} = \Gamma_R(-E_c)\frac{\Gamma_L(E_c)}{\Gamma_L(E_c)+\Gamma_R(E_c)} + \Gamma_L(-E_c)\frac{\Gamma_R(E_c)}{\Gamma_L(E_c)+\Gamma_R(E_c)}. \quad (7)$$

We note that the sequences where an electron tunnels to the turnstile island and then back are too fast to be detected and hence do not affect the observed hold times. Furthermore, the charging energy of the trapping node is considered to be compensated in the experiment by an appropriate bias voltage V_b, and it was not included in the simulations.

Figure 10 demonstrates reasonable agreement between the measured and calculated hold times in the trap. The parameters used in numerical calculations are summarized in table 3. The fit value of $E_c = 600\,\mu$eV in sample 1 is lower than its experimental estimate $E_c \approx 750\,\mu$eV, which we attribute to the effect of a not quite optimal gate voltage setting in measurements. The fit value of $R_{4.2\,K}$ for sample 1 was found larger than that of sample 2 by a factor of 6.3, corresponding to a factor of $\sqrt{6.3} \approx 2.5$ in the voltage fluctuation amplitude. Larger voltage fluctuations can be, at least partially, attributed to the lower junction capacitance of sample 1 compared to sample 2 (see table 2). Furthermore, since the photon energy E_{ph} required to overcome the Coulomb blockade barrier is different for the two samples, any deviation of the true noise spectrum from the assumed first-order decay could also result in different fit values for $R_{4.2\,K}$.

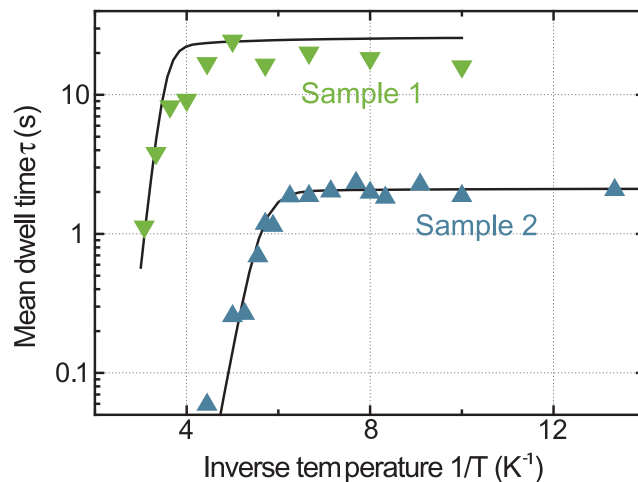

Figure 10. The experimental hold times (filled symbols, shown previously in figure 7) versus the results for the two-fluctuator model (black curves).

At higher temperatures, the hold times are influenced by the thermal broadening of the Fermi factors, but also by an increased probability of photon emission by the on-chip resistor (see the plot P versus E for $E < 0$ in figure 9). For sample 1, we evaluated the hold time also in the case of a magnetically suppressed energy gap $\Delta = 0$. The obtained value of 4.5 s is to an order of magnitude consistent with the experimental hold time $\tau \sim 10\,\mathrm{s}$ (see figure 5), which provides one more proof of validity for our model.

5. Conclusions and outlook

Our study of the hold times in the two-junction hybrid R-traps gives rise to a promising prediction of the leakage-limited pumping accuracy of hybrid R-turnstiles. The hold times on the scale of up to tens of seconds imply that the metrological accuracy is feasible and could, in principle, be realized with the help of a special rectangular drive [10]. A more detailed study is under way to characterize the leak in the gate-open state of the turnstile, which is relevant to a more common sinusoidal driving signal. The experimental switchings have been successfully interpreted in terms of the environmentally induced escape processes. In particular, good agreement has been achieved in the frame of a two-component model of the environment. Significant disturbances have been shown to arrive from the warmer parts of the setup, supposedly from outside the sample stage. In this respect, an important further insight can be provided by comparing the hold times of the same trapping device, measured in different measurement setups or by varying the quality of noise filtering.

Acknowledgments

Fruitful discussions with S Kafanov and V Bubanja are gratefully acknowledged. Technological support from T Weimann and V Rogalya is appreciated. This research, conducted within the EU project SCOPE, received funding from the European Community's Seventh Framework Programme under grant agreement no. 218783.

References

[1] Averin D V and Likharev K K 1991 *Mesoscopic Phenomena in Solids* (Amsterdam: Elsevier) pp 173–271
[2] Geerligs L J, Anderegg V F, Holweg P A M, Mooij J E, Pothier H, Esteve D, Urbina C and Devoret M H 1990 *Phys. Rev. Lett.* **64** 2691
[3] Pothier H, Lafarge P, Orfila P F, Urbina C, Esteve D and Devoret M H 1991 *Physica* B **169** 573
Pothier H, Lafarge P, Urbina C, Esteve D and Devoret M H 1992 *Europhys. Lett.* **17** 249
[4] Pekola J P, Vartiainen J J, Möttönen M, Saira O-P, Meschke M and Averin D V 2008 *Nat. Phys.* **4** 120
[5] Averin D V and Odintsov A A 1989 *Phys. Lett.* A **140** 251
Averin D V and Nazarov Yu V 1990 *Phys. Rev. Lett.* **65** 2446
[6] Averin D V and Pekola J P 2008 *Phys. Rev. Lett.* **101** 066801
[7] Kautz R L, Keller M W and Martinis J M 2000 *Phys. Rev.* B **62** 15888
[8] Pekola J P, Maisi V F, Kafanov S, Chekurov N, Kemppinen A, Pashkin Yu A, Saira O-P, Möttönen M and Tsai J S 2010 *Phys. Rev. Lett.* **105** 026803
[9] Keller M W, Eichenberger A L, Martinis J M and Zimmerman N M 1999 *Science* **285** 1706
[10] Kemppinen A, Kafanov S, Pashkin Yu A, Tsai J S, Averin D V and Pekola J P 2009 *Appl. Phys. Lett.* **94** 172108
[11] Maisi V F, Pashkin Yu A, Kafanov S, Tsai J S and Pekola J P 2009 *New J. Phys.* **11** 113057
[12] Odintsov A A, Bubanja V and Schön G 1992 *Phys. Rev.* B **46** 6875
[13] Golubev D S and Zaikin A D 1992 *Phys. Lett.* A **169** 475
[14] Zorin A B, Lotkhov S V, Zangerle H and Niemeyer J 2000 *J. Appl. Phys.* **88** 2665
[15] Lotkhov S V, Zangerle H, Zorin A B and Niemeyer J 1999 *Appl. Phys. Lett.* **75** 2665
[16] Lotkhov S V, Bogoslovsky S A, Zorin A B and Niemeyer J 2001 *Appl. Phys. Lett.* **78** 946
[17] Dresselhaus P D, Ji L, Han S, Lukens J E and Likharev K K 1994 *Phys. Rev. Lett.* **72** 3226
[18] Krupenin V A, Lotkhov S V and Presnov D E 1997 *J. Exp. Theor. Phys.* **84** 190
[19] Dynes R C, Garno J P, Hertel G B and Orlando T P 1984 *Phys. Rev. Lett.* **53** 2437
[20] Lotkhov S V, Kemppinen A, Kafanov S, Pekola J P and Zorin A B 2009 *Appl. Phys. Lett.* **95** 112507
[21] Saira O-P, Möttönen M, Maisi V F and Pekola J P 2010 *Phys. Rev.* B **82** 155443
[22] Dolan G J 1977 *Appl. Phys. Lett.* **31** 337
Niemeyer J 1974 *PTB-Mitt* **84** 251
[23] Lotkhov S V, Camarota B, Scherer H, Weimann T, Hinze P and Zorin A B 2009 *Proc. IEEE Nanotechnology Materials and Device Conf.* (*Traverse City, USA*) pp 23–6
[24] Fulton T A, Gammel P L and Dunkleberger L N 1991 *Phys. Rev. Lett.* **67** 3148
[25] Lafarge P, Joyez P, Pothier H, Cleland A, Holst T, Esteve D, Urbina C and Devoret M H 1992 *C. R. Acad. Sci. Paris* **314** 883
[26] Martinis J M, Nahum M and Jensen H D 1994 *Phys. Rev. Lett.* **72** 904
[27] Maibaum F, Lotkhov S V and Zorin A B 2011 in preparation
[28] Ingold G L and Nazarov Yu V 1992 *Single Charge Tunneling, Coulomb Blockade Phenomena in Nanostructures* (*NATO ASI Series B* vol 294) (New York: Plenum) chapter 2
[29] Farhangfar Sh, Toppari J J, Pashkin Yu A, Manninen A J and Pekola J P 1998 *Europhys. Lett.* **43** 59
[30] Farhangfar Sh, Manninen A J and Pekola J P 2000 *Europhys. Lett.* **49** 237
[31] Ingold G-L, Grabert H and Eberhardt U 1994 *Phys. Rev.* B **50** 395